Materials Transactions, Vol. 55, No. 12 (2014) pp. 1806 to 1815

Quantitative Nondestructive Evaluation of Plastic Deformation in Carbon Steel Based on Electromagnetic Methods

Hong-En Chen[1], Shejuan Xie[1], Zhenmao Chen[1,*], Toshiyuki Takagi[2], Tetsuya Uchimoto[2] and Kensuke Yoshihara[3]

[1]*State Key Laboratory for Strength and Vibration of Mechanical Structures, Xi'an Jiaotong University, 710049, China*
[2]*Institute of Fluid Science, Tohoku University, Sendai 980-8577, Japan*
[3]*The Kansai Electric Power Co., Mikata-gun, Fukui 919-1141, Japan*

Plastic deformation may occur in a mechanical structure during its manufacturing and service process, and may cause serious problem in the structural integrity. Therefore, a reliable pre-service or in service quantitative non-destructive evaluation (NDE) of plastic deformation is very important especially for a structure after suffering giant load such as a large earthquake. However, there is still no satisfactory method being established for the quantitative NDE of plastic deformation in key structures such as those of a nuclear power plant. For this purpose, three electromagnetic NDE methods, i.e., Magnetic Barkhausen Noise (MBN), Magnetic Incremental Permeability (MIP) and Magnetic Flux Leakage (MFL) method are studied via experiments in this paper to investigate their feasibility for evaluation of plastic deformation in carbon steel SS400. A special testing system integrated these three electromagnetic NDE methods is established to measure the magnetic property of test-pieces with different plastic deformation, which was introduced by a tensile testing machine. It is found that the measurement signals of all these three methods have clear correlation with the plastic strains and show coincident tendency, which reveals the validity of these methods for the quantitative evaluation of plastic deformation. Among these methods, the MFL signals are of higher stability and repeatability but of relative low spatial resolution. The MBN method can give better resolution but of bigger standard deviation and is also not valid to evaluate a plastic strain of large scale. On the other hand, the MIP signals are more sensitive to the liftoff of sensor and to the remanent magnetization status, i.e. of more noise. Therefore, to measure the feature parameters of these three methods at the same time with an integrated testing system and to evaluate the plastic strain through signal fusion may give a better detectability and evaluation precision. [doi:10.2320/matertrans.M2014173]

(Received May 22, 2014; Accepted September 16, 2014; Published November 25, 2014)

Keywords: *plastic deformation, carbon steel, Barkhausen noise, magnetic incremental permeability, magnetic flux leakage*

1. Introduction

As one of the most popular materials, carbon steel is widely used in many engineering fields such as nuclear power plant, railway and gas pipelines etc. Plastic deformation and residual stress always arise in a structural component of carbon steel during its manufacture and service process due to unexpected load such as a large earthquake. Plastic deformation may seriously reduce the material fatigue strength and fracture toughness, and consequently cause structural safety problem. To ensure the structural integrity after an unexpected loading process, quantitative nondestructive evaluation (NDE) of plastic deformation and residual stress is very important.

Plastic deformation in crystal structures is a kind of micro-defects, such as slip lines and dislocations, consequently may affect the orientation and irreversible movement of magnetic domain wall in a ferromagnetic material. The orientation and irreversible movement of magnetic domain wall give significant influence on the magnetic material property such as permeability, coercive force, and even cause perturbation to the magnetic field surrounding the material. This gives a good possibility to conduct quantitative NDE of plastic deformation in the carbon steel by measuring and extracting signal feature parameters related to the material magnetic properties.

Several NDE methods in electromagnetic category have been proposed and their performances were investigated aiming at quantitative evaluation of the plastic deformation or residual stress in a structural component. Among them, the Magnetic Barkhausen Noise (MBN) method is the most attractive method being studied in term of objective material, signal feature parameter,[1–4] measurement system and interaction mechanism etc.[4–8] The evaluation of plastic deformation by using Metal Magnetic Memory (MMM) method is studied by many researchers.[9–12] In addition, some other new methods such as nonlinear eddy current testing method[13–15] are also evaluated for the NDE of the plastic deformation. However, there are still problems limited the application of these methods such as the uncertain feature of the measurement results. The uncertainty may be caused by experimental conditions and also the material batch, surface quality, heat treatment and grain structure etc. Due to such complicity to evaluate the plastic deformation/residual stress, multi-parameters and hybrid-methods to make comprehensive evaluation are required in order to get more reliable evaluation results. The methodology of micro-magnetic, multi-parameter, micro-structure and stress analysis (3MA technology) was developed by the research group in the Fraunhofer IZFP in order to characterize mechanical material properties such as the hardness, hardening depth, yield and tensile strength[16] etc. The micro-magnetic NDE techniques of MBN, the Magnetic Incremental Permeability (MIP) and the harmonic analysis of the tangential magnetic field are mainly applied in the 3MA technology.

Magnetic Barkhausen noise is generated when the moving magnetic domain walls break through pinning points of micro-defect such as dislocation and slip lines. MBN signals directly reflect the movement and orientation states of the magnetic domains that closely relate to the material micro-structures. Therefore, there is a possibility to apply MBN to evaluate the residual plastic deformation, residual stress, and

*Corresponding author, E-mail: chenzm@mail.xjtu.edu.cn

Table 1 The chemical composition of SS400 carbon steel (mass%).

C	Mn	Si	S	P	Fe
0.15	0.42	0.02	0.007	0.014	bal.

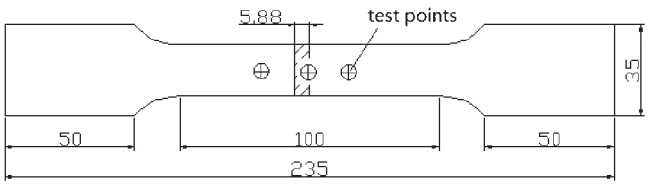

Fig. 1 The shape and dimensions of specimens (Unit: mm).

ferrite content etc. in a material. On the other hand, the MIP is defined as the average slope of the minor hysteresis loop generated by an alternating magnetic field of amplitude smaller than the magnetic coercive force at different point of the major hysteresis loop.[17,18] The MIP can reflect the reversible magnetization information through its profiles feature parameters during the whole magnetization and demagnetization procedure, and consequently is considered as a good index of the plastic deformation. In addition, the perturbation information of the leakage magnetic field surrounding the specimen surface measured by the Magnetic Flux Leakage (MFL) method is also closely correlated with the states of orientation and irreversible movement of magnetic domains caused by the plastic strains in a ferromagnetic material. Though these methods are fully adopted in the 3MA technology for evaluation of residual stress and hardness, their feasibility and efficiency for evaluating the plastic deformation in carbon steel is not clarified yet.

In this paper, the correlations of plastic deformation with NDE signals of the MBN, MIP and the MFL method are investigated via experiments for the carbon steel SS400, which is widely used in nuclear power plants (NPPs). The feasibilities of each method are investigated and their efficiencies are compared. In addition, the interaction mechanism between the plastic deformation and the magnetic property is also discussed from the view point of the microstructure and the movement of magnetic domain to understand the measurement results. The possibility to enhance the detectability of plastic deformation by using the hybrid method is also discussed.

2. Methods and Experimental Details

2.1 Testing material, specimens and loading conditions

Aiming to evaluate the plastic strain in NPP structural components after a large earthquake, a major structural material of the NPPs in Japan, i.e., the carbon steel SS400 (JIS), is taken as the testing material in this study. The chemical composition of the SS400 carbon steel is listed in Table 1. In order to minimize the influence of the initial micro defect, heat treatment (keeping one hour at 500°C temperature condition) is carried out to anneal the TPs before introducing plastic deformation.

Five plate test-pieces (TP) of 5.88 mm thickness of design shown in Fig. 1 are fabricated. Uniform plastic strains are applied to the measurement range (central part of 100 mm length) of the TPs by tensile testing. As only tensile loading is considered, the length of the TP is selected relative big as a larger TP is more convenient to make the electromagnetic NDE measurements of this study. Different levels of residual plastic strains (0%, 1%, 2%, 3% and 5%) are applied to the specimens respectively by stretching the TP to a large strain with a MTS testing machine at a strain rate of 0.1 mm/min and unloading it then for measurement. The strain of TP is monitored by an extensometer (gauge length 25 mm and travel 20 mm) and a strain gauge mounted on the sample during the tensile testing.

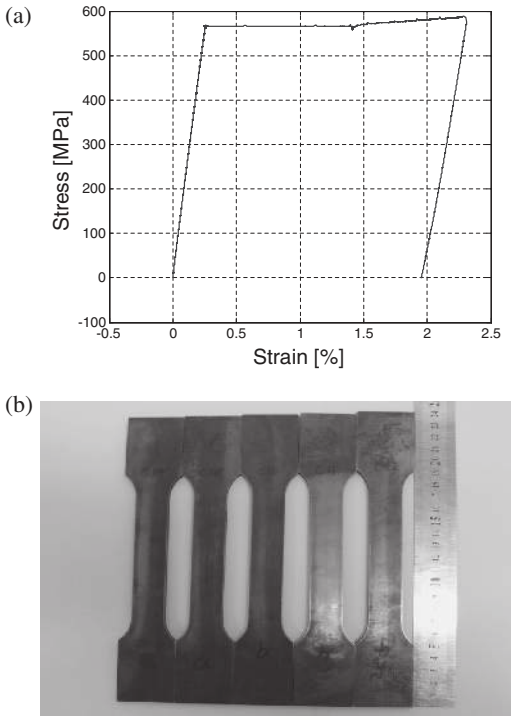

Fig. 2 Typical loading process and a picture of TPs after plastic deformations being introduced. (a) The stress-strain loading process of TP2; (b) The TPs after plastic strain of 0%, 1%, 2%, 3% and 5% are loaded.

Figure 2(a) shows the loading process of the TPs in term of strain-stress curve. When the force is unloaded, i.e., zero stress state, the remained strain value is the residual strain in the TP. Considering the shape of the TP and loading process, the macro-strain at the central part of the TP is basically uniform. The picture of TPs after plastic deformation is given in Fig. 2(b). The TPs are named as TP1, TP2, TP3, TP4 and TP5 from the left to right in Fig. 2(b). The change of TP length even can be observed from the figure directly.

2.2 Integrated testing systems for measurement of MBN, MIP and MFL signals

The MBN, MIP and MFL measurement systems have several similar components, e.g., an electromagnetic (EM) magnet to apply static or quasi-static magnetic field to magnetize the testing material. On the other hand, the pickup units of these methods are different from each other. A coil is usually adopted to pick up the MBN signal by setting it near

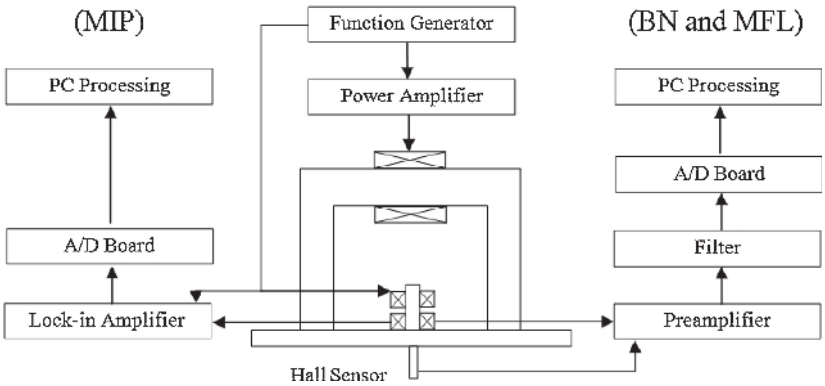

Fig. 3 Integrated measurement system for magetic Barkhausen noise, magnetic flux leakage and magnetic incremental permeability method.

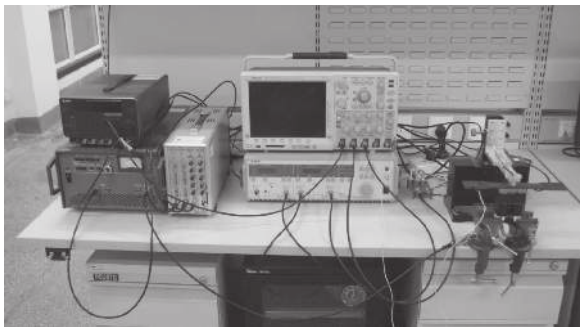

Fig. 4 Photography of the integrated experimental system for MBN, MIP and MFL measurement.

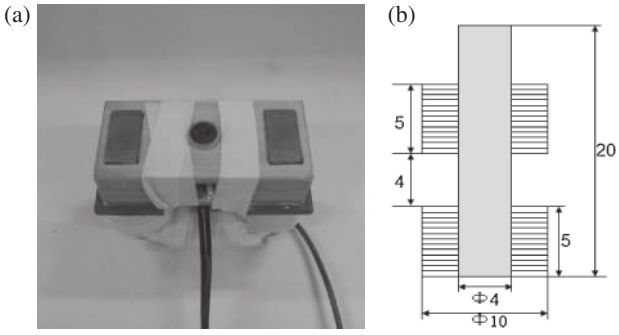

Fig. 5 The probe of integrated experimental system and parameters of pick-up coils. (a) The photography of electromagnetic magnet and pick-up probe; (b) the design and parameters of the pick-up coils.

by the surface of TPs, while an ECT probe consisting both exciting coil and pickup coil is necessary to measure MIP signals once low frequency magnetic field is applied to the TP with the EM magnet. On the other hand, a magnetic sensor is usually utilized to measure the MFL signals. Integrating these 3 measurement systems is a good way to simplify the testing system and realize simultaneous measurements of the MBN, MIP and MFL signals.

The block diagram and photography of the integrated MBN, MFL and MIP measurement systems are shown in Fig. 3 and Fig. 4. The MBN, MIP and MFL inspection systems share the same EM magnet unit that consists of a function generator, a power amplifier, U shaped permalloy yoke and a group of excitation coils wounded on the yoke. Function generator provides sinusoidal exciting signals of frequency less than 1 Hz, and the signal is amplified by a power amplifier to provide strong current to drive the exciting coil of the EM magnet. The EM magnet is attached on one side of the specimen to magnetize the TP along its length direction and generate different magnetic status. On the other hand, a pick-up unit consisting of two coaxial coils and a Hall sensor is designed and fabricated to measure the MBN, MIP and MFL signals. As shown in Fig. 5, a mutual induction ECT probe with a cylindrical magnetic core is adopted for the MBN and MIP measurements. The top coil of the ECT probe (far from TP) is selected as the excitation coil and the bottom coil (near TP) is the pickup element. In case of MBN measurement, only the pickup coil of the ECT probe is used to measure the high frequency noise signal while both the excitation and the pickup coils are necessary for the MIP measurement to obtain both the real and imaginary response of the ECT probe. From this point of view, though the MIP and MBN testing system are integrated together in Fig. 1, the MIP and MBN testing have to be carried out separately. On the other hand, the MFL signals can be measured during the MIP or MBN testing procedure as the pickup element is independent (Hall sensor).

2.3 Testing principle and procedure

2.3.1 MBN method

The ferromagnetic material contains lots of magnetic domains in which the orientations of easy axis are consistent each other. When an external magnetic field is applied, the magnetic domains may show reversible and irreversible motions during the magnetization and demagnetization procedure. The sudden irreversible motion of magnetic domains causes a pulsed change in magnetic field, which is known as magnetic Barkhausen noise when measured by a magnetic sensor or coil.

The total MBN signals imply status of the micro-defects (e.g., plastic deformation) in material. The emission of MBN signals is considered caused by the release of the accumulated energy when movement of the magnetic domains overcomes the obstacles. Because the resistance of obstacles and size of domains are inhomogeneous, the amplitude of emitted pulsed magnetic field is different. On the other hand, as the easy magnetization axis and movement angle are non-directional, the MBN signals may have both positive and

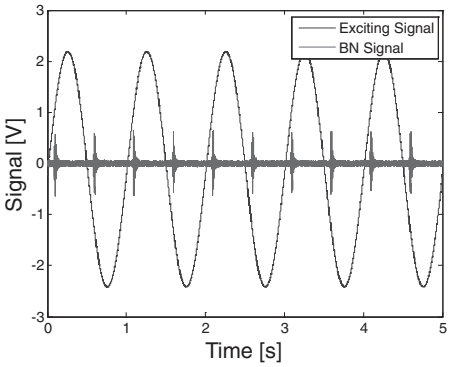

Fig. 6 MBN signals and exciting signals without plastic deformation.

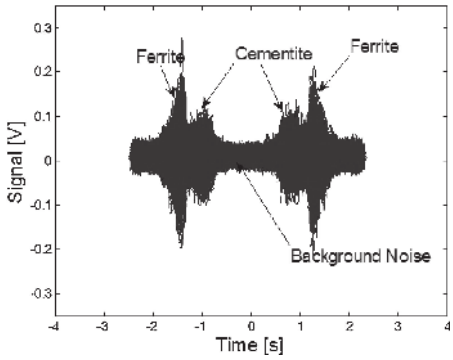

Fig. 7 The threshold for the BN signals.

negative values. Higher amplitudes of MBN signals imply bigger sizes of obstacles and magnetic domains.

In this study, the MBN signal is measured by using a pick-up coil of 1000 turns (bottom coil in Fig. 5(b)) and with a ferrite core. The MBN signals from pick-up coil are amplified by 2000 times, filtered with a band pass filters (500 Hz∼ 100 kHz), and finally are digitized and memorized by an oscilloscope and a computer.

A typical MBN signal of the SS400 specimen without plastic deformation (TP1) is shown in Fig. 6 where how the MBN signals occur during the magnetizing process is illustrated. There are two kinds of signals in the Fig. 6, one is sinusoidal that is the driving signal of the EM magnet, and the other is the MBN signals of the apparent pulses measured by the coil. One period of the excitation magnetic field and the response magnetization forms a hysteresis loop. A completed hysteresis loop consist of magnetization process and reverse magnetization process, which cause two groups of MBN signals in one excitation period (Fig. 6). The peak of MBN signals appears at the steepest region of the hysteresis loop, which corresponds to the coercivity points.

The MBN signals contain 3 kinds of feature signals, i.e., background noise, signal due to ferrite phase, and signal due to cementite. In Fig. 7, there are two peaks in each group of MBN signals, the lower peak depends on the content of cementite and the higher peak is caused by ferrite phase.[19] Though the micro-defect information is included in the MBN signals, a proper signal index is very important to correlate the defect information and the signal. Index values (feature parameter of MBN signals) such as the "Energy" of the MBN signal have been proposed. The background noise and signal from cementite in MBN signals may give big influence on the feature parameters. In practice, a threshold value is usually selected to get rid of them, i.e., to eliminate the influence of cementite phase and background noise. Because the peaks of MBN signals are ragged during different circles of magnetizing process, the "Energy" is used as the average value to reflect the change of the MBN signal intensity with the plastic deformation. After the "Energy" being calculated, the attenuation ratio of MBN signals is extracted by normalizing the calculated values in order to evaluate the plastic deformation quantitatively.

In this work, the Energy of MBN defined by the following formula is adopted:

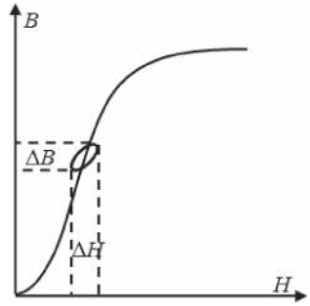

Fig. 8 Concept diagram of the magnetic incremental permeability.

$$MBN_{\text{energy}} = \sum_{\text{i}} \int_{s_{\text{i}}}^{e_{\text{i}}} u^2(t)\mathrm{d}t \tag{1}$$

Here s_{i} is the start time of signals, e_{i} is the end time of the i-th segment of MBN signals, and $u(t)$ is the voltage value of the measured MBN signals. To normalize the index parameters, the values obtained for the TP without plastic deformation are set as "1", i.e. the values of TPs of different plastic deformation are divided by this reference value.

2.3.2 MIP method

As shown in Fig. 8, magnetic incremental permeability is defined as the gradient of the minor loops which is superimposed onto a major hysteresis curve, i.e., the minor loops are generated in process when the material is magnetized and demagnetized by a large magnetic field.[17] In practice, the EM magnet with a driven current of low frequency is used to magnetize the material to different point at the major loop and an ECT probe of high frequency is used to generate the minor loop and to measure its gradient that is corresponding to the MIP value. The phase information of the ECT signals included in the real and imaginary values of the MIP signals is also important for the material characterization.

As a magnetic material parameter, the MIP depends on the reversible magnetization in magnetic material, which is closely correlated to the microstructure of the ferromagnetic material. In this study, in addition to the EM magnet used for MBN to magnetize the material, an ECT probe with two coaxial coils is adopted to measure the MIP values by setting it at the material surface and between the yoke legs of the EM magnet (see Fig. 5). The coil of the ECT probe relatively far from the inspection target (top coil) is the excitation coil that is driven by a function generator to produce a high frequency

eddy current in the ferromagnetic specimen. As the coil size and the driving current are small, the amplitude of the magnetic field generated by the excitation coil is much smaller than the coercivity of the material, which enables the generation of the local minor loop. To make the distinction of the magnetic field of the EM magnet and the ECT probe easier, very different frequencies are adopted for the EM magnet and the ECT probe respectively, e.g. 1 Hz for EM magnet but 10 kHz for the ECT probe.

On the other hand, the coil of the ECT probe near the specimen (bottom coil) is used to pick-up the information of the high frequency eddy current. Both the real and imaginary parts of the ECT signals are measured with a lock-in amplifier, which are processed then to obtain the MIP values. In practice, as the real part V_R and imaginary part V_i of the ECT pickup signals are in proportion to the ΔB inside the material, and the total current of amplitude I in the excitation coil is in proportion to the applied magnetic field ΔH, the real and imaginary part of the relative MIP value can be calculated by

$$\mu_{\Delta R} = V_R/I, \quad \mu_{\Delta i} = V_i/I \tag{2}$$

here $\mu_{\Delta R}$ and $\mu_{\Delta i}$ are relative MIP values that are only different from the practical MIP values in scale. The ratio between these values and the practical MIPs is the same for all the applied magnetic field. Therefore, $\mu_{\Delta R}$ and $\mu_{\Delta i}$ are suitable to be taken as MIP values for the NDT application.

The MIP is correlated to the magnetization state of the material when it is measured, i.e. it depends on the amplitude of the driving current in the EM magnet for magnetizing the material. If we take the driven current as the horizontal axis and the MIP value as the vertical axis, a butterfly like I-μ loop can be plotted. However, as the MIP correlate to the magnetization status in the material directly, taking the magnetization status near by the ECT probe as the horizontal axis of MIP loop is more reasonable to describe the dependence of MIP on the local magnetic material property. In view of this point, the tangential magnetic field signal near by the surface of test-piece, which is the leak field due to the magnetization inside the material, is measured and taken as the horizontal axis to plot MIP profile curve. In this way, typical butterfly MIP profile, such as that shown in Fig. 9, can be obtained, and their feature parameters can be used to characterize the material degradation.

During the measurement, the current in the EM magnet is of 1 A amplitude and 1 Hz frequency, while the voltage amplitude of the driving current of ECT probe was set as 2.5 V and the frequency was 10 kHz. The TPs with different plastic deformation are measured respectively in a stable environment, and the results are presented in the next section.

2.3.3 MFL method

While the irreversible motion information can be acquired by the MBN, the MFL signals, which are caused by the magnetization in the material, may contain other information related to the non-linear magnetic material property. For this reason, the MFL signals are also measured and evaluated in this study.

The measurement procedure of MFL signals is quite similar to that for the MBN signal measurement. Instead of using a pickup coil to measure the induction voltage due to magnetic field of MBN perpendicular to the TP surface, a Hall sensor is set between the yoke legs to measure the value of the magnetic field parallel to the TP surface. As this MFL signal is of the magnetic field parallel to the surface, it is also called the tangential magnetic field and known as a good index parameter to describe the magnetic material status.[16)]

For practical measurement of MFL signals, the EM magnet for MBN system with same driving current (amplitude and frequency) is adopted again. A Hall magnetic sensor is set at the center point between the two yoke legs and in parallel to the TP surface with a special fixture (Fig. 3 and Fig. 4) to measure the tangential magnetic flux leakage field. As the output of the Hall sensor is not small and it changes slowly (1 Hz), it is measured by using an A/D board and is memorized in the data acquisition computer for further processing.

A typical tangential magnetic field signal measured with a TP of virgin material is shown in Fig. 10. There are super-harmonic distortions apparently in the tangential magnetic field signals for the applied exciting signal of simple sinusoidal wave. The distortion times are closely related to the emission point of MBN signals, i.e., nearby the coercivity points of the hysteresis loop. This means that, the strong movement of magnetic domains near the coercivity points may not only cause MBN field, but also cause a strong magnetization, and consequently, a nonlinear change of magnetic field outside the material, i.e. the super-harmonic components in the MFL signals. As the movement of magnetic domains can be influenced by the microstructure of material, this distortion can be a good index to evaluate the

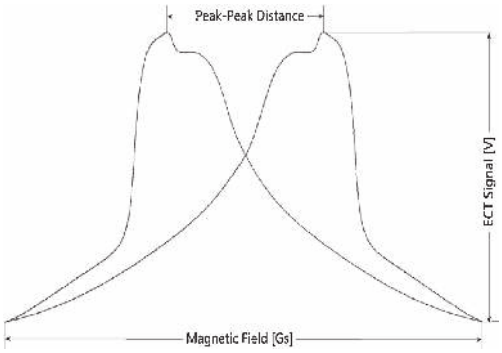

Fig. 9 Typical butterfly MIP profile and feature parameters.

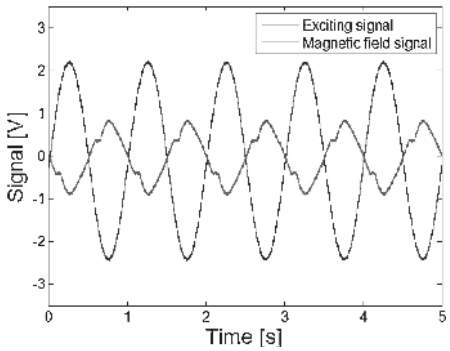

Fig. 10 Typical tangential magnetic field signals and exciting signals for TP without plastic deformation.

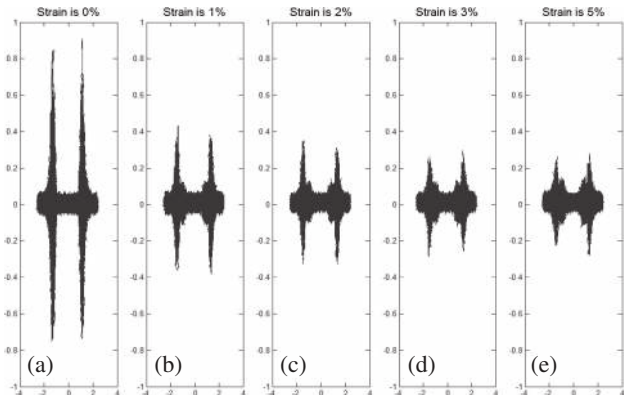

Fig. 11 MBN signals for TPs of plastic deformation of 0% (a), 1% (b), 2% (c), 3% (d), 5% (e).

microstructure change due to micro-defect such as the plastic deformation.

In order to extract the feature of distortions in the MFL signals, which is usually in form of super-harmonic waves, spectrum analyses are performed to the measured tangential magnetic field signals. The amplitude of odd harmonics such as 3rd, 5th, and 7th harmonics are taken as the feature parameters of the signals. In addition, to cover all the super-harmonic energy, K factor, which is defined by Dobmann etc.[16] is also calculated. As given in eq. (3), the K factor is defined as the geometrical average (root-mean-square-value) of the power of the super harmonic components, and normalized to the power of the fundamentals,

$$K = \sqrt{\frac{A_3^2 + A_5^2 + A_7^2 + A_9^2}{A_1^2}} \tag{3}$$

here, A_1, A_3, A_5, A_7, A_9 are the amplitude of fundamental, 3rd, 5th, 7th and 9th harmonics, respectively.

3. Measurement Results

3.1 Results of MBN method

Figure 11 shows typical MBN signals for TPs with different level of residual plastic deformation for measurement point at the TP center. The other signals measured near by the center point and from the other side are of same feature with those shown in Fig. 11. The testing conditions for all the TPs are the same, i.e., the conditions shown in the section 2. From the figure, one can find that the peaks of MBN signal decrease abruptly for TPs with and without plastic deformation (0% to 1%). The reduction of the signal amplitudes, however, becomes slower for relatively large plastic deformation. For a large plastic deformation such as those over 3%, the reduction is very small. On the other hand, the signal which is caused by the phase of cementite (the small peak shown in Fig. 11) gradually became stronger for a large plastic deformation. For this reason, different threshold signal values are necessary to process the raw MBN signals such as those given in Fig. 11 and to extract the MBN feature parameters.

Figure 12(a) shows the correlation of the MBN energy of the measured MBN signals with the residual plastic strain in test-pieces. Six points are measured for each test piece and

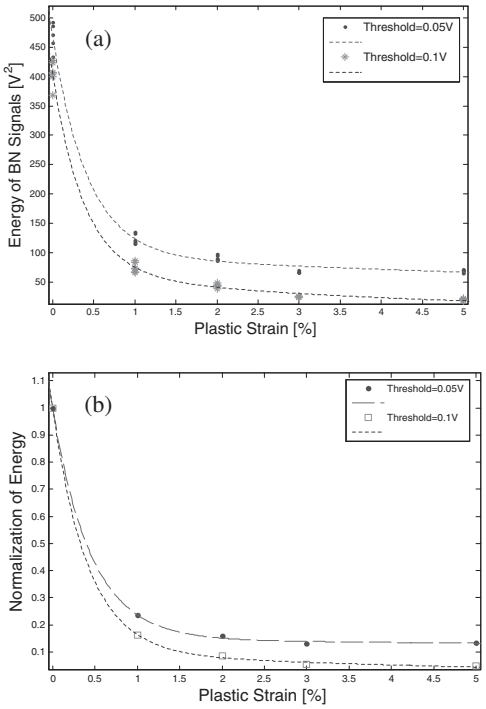

Fig. 12 Dependence of MBN Energy on the plastic strain for threshold values of 0.1 V and 0.05 V.

the extracted feature parameters are plotted in the figure. On the other hand, Fig. 12(b) gives the results of the normalized MBN energy values. Only the normalized average values are given in this case. The MBN energy shows that the feature parameter values decrease rapidly at a low plastic deformation range and get saturated gradually with increasing plastic strain. In addition, the results of different threshold value for calculating the feature parameter have similar exponential attenuation relationship with plastic strain.

The measurement resolution is about 4 mm for the MBN signal measurements, which is related to the size of pick-up coil, i.e., the measured signals are basically averages of information around the probe. However, as the plastic deformation of the test-piece at measurement zone is basically uniform in this study, the measured signals also represent the local information of plastic deformation in the test-pieces. The same thing is also valid for the MIP and MFL methods.

However, one can find from Fig. 12 that the correlation when threshold is set as the peak value of cementite phase noise (0.1 V) is more sensitive to the plastic strain than that of threshold 0.05 V (amplitude of background noise). When the threshold is set as the value of background noise (0.05 V), the energy of MBN signals is almost unchanged for plastic strain exceeding 2%, while the energy decays from 0.1 to 0.04 for plastic strain range 2% to 5% when the threshold is set as 0.1 V.

The phenomena just described above can be well explained from the microstructure point of view. In fact, the microstructure in form of grain boundary, dislocation and second phase material interferes with motions of magnetic domain. According to the principle of MBN, the domains accumulate energy at the pinning points during magnetization process, and the accumulated energy will be released and

caused emission of a pulsed EM field after passing the pinning site. The more impediments of domain motions, the smaller amplitude of MBN signals emission. At low level plastic strain, grains are fragmentized by plastic damage, and the hardness of material is enlarged. Smaller grain boundary size leads to more, but smaller amplitude of MBN emissions. Therefore, the peak and RMS of MBN signals decrease with the plastic deformation rapidly in range of a small plastic strain. At the same time, a larger hardness weakens the MBN activity, and causes the reduction of the MBN Energy.

On the other hand, microstructure varies from isolated dislocation to dislocation cells of high density in case of a relative larger plastic strain. The dislocations of high density become a stronger pinning site with high energy. If no enough energy is supplied to domains to overcome these strong pinning sites, the MBN signal level will be weaken and gradually saturated at last. These explanations reveal that the measurement results of MBN shown in Fig. 11 and 12 are reasonable. In other word, energy of MBN signal is suitable as the index parameter for quantitative evaluation of plastic deformation in SS400 material, and the cementite threshold value of noise level (0.1 V) is better for extracting the feature parameter of MBN signals for the plastic strain assessment.

3.2 Results of MIP method

Figure 13 shows the measured MIP profiles for TPs with residual plastic strain of 0%, 1%, 2%, 3% and 5% respectively, where the ECT signals which are in proportion to the MIP values are plotted as the vertical axis. The profile shown in Fig. 13 is just of same geometry with practical MIP–magnetization intensity correlation. It is not difficult to find from the figure that the feature parameters of the measured MIP profiles, such as the peak value, the area and the peak to peak distance changes with the status of residual plastic strain in the TPs. The MIP profiles of the imaginary part shows more difference than the real part, and MIP of virgin material is significantly different from TPs with plastic strain. These results reveal that all the feature parameters can be adopted to evaluate the plastic deformation. In this paper, the peak value of MIP profile is selected as the index to evaluate the plastic strains.

Figures 14 and 15 show the correlations of the MIP peak values with plastic strain, with (a) gives the dependence of peak values on the plastic strain, and (b) gives the normalization peak values. In Fig. 14(a) and 15(a), the results at different measurement points are plotted while only the average values are given in the Fig. (b). The average peak values are normalized by subtracting the measured values with that of the virgin material. Both the results of the real and imaginary MIP peak values show an exponential dependence on the plastic strains. From the normalized results, the peak values of real MIP real part are in a range from 0.17 to 0.18 for the plastic strain of 1% to 5%, while the peak values of the imaginary MIP change from 0.24 to 0.34 with the same plastic strain range. In other words, the imaginary MIP is more suitable for quantitative evaluation of the plastic strain.

To explain the measured MIP results, the movements of magnetic domains need to be considered again. As the domain movement becomes more difficult due to an

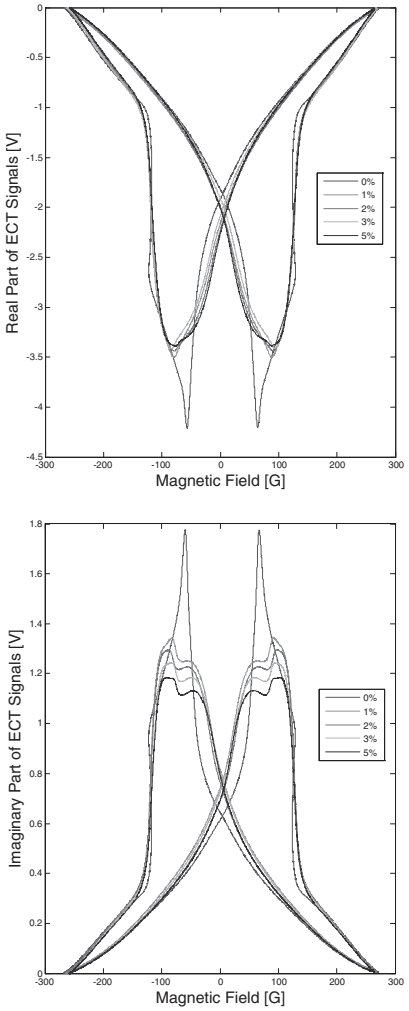

Fig. 13 Profiles of incremental permeability with different plastic strains.

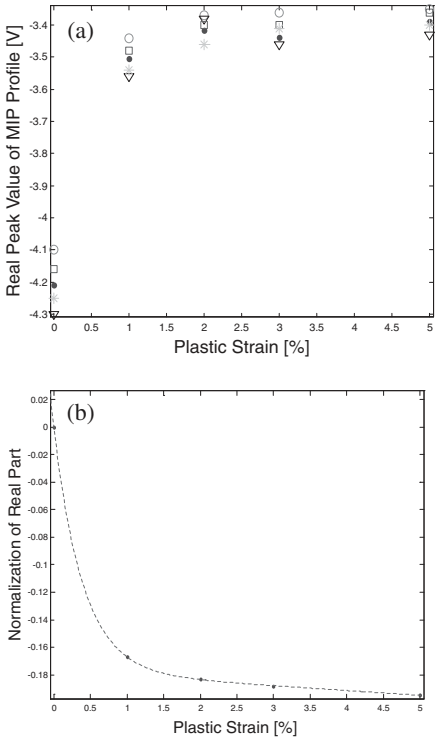

Fig. 14 Correlation of peak values of MIP real part with plastic strain. (a) Measured values, (b) normalized values.

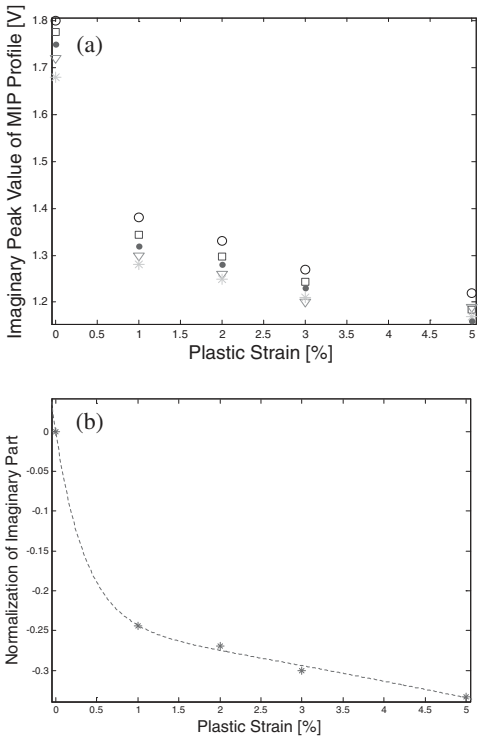

Fig. 15 Correlation of peak values of MIP imaginary part with plastic strain. (a) Measured values, (b) normalized values.

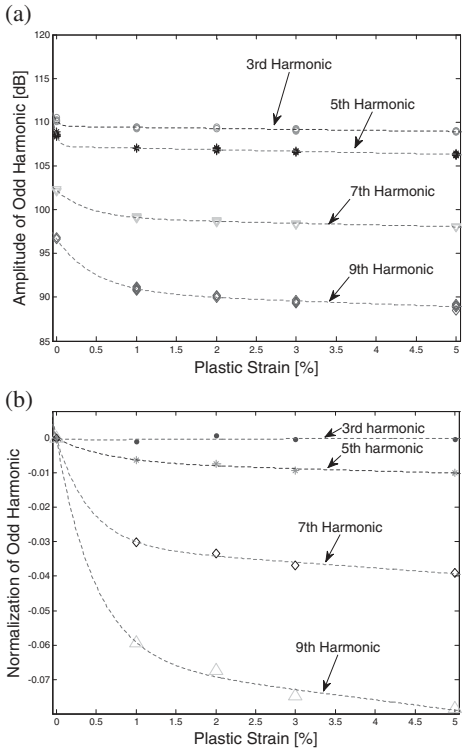

Fig. 17 Correlations of amplitude of odd harmonics with plastic strain.

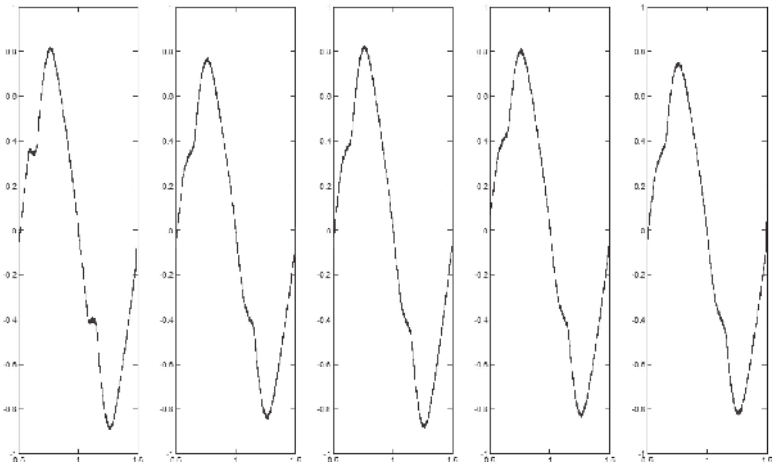

Fig. 16 MFL signals for TPs of plastic deformation of 0%, 1%, 2%, 3%, 5%.

increasing plastic deformation, the reversible magnetization will also become smaller, which may influence the MIP value at the coercivity point more significantly. The MIP measurement results also imply that the maximum permeability decays with the plastic strain as shown in Fig. 13 to 15. This is because that the orientation change and irreversible movement of magnetic domains may affect the electromagnetic parameters, e.g., permeability, and cause magnetic field perturbation consequently. The MIP results shown in this subsection are similar to that of the MBN results. Both results imply that the plastic deformation makes impediments to the movement and rotation of magnetic domains.

3.3 Results of MFL method

Figure 16 gives the original MFL signals for TPs with different residual plastic strains. Figure 17 shows the correlation of amplitude of 3rd to 9th odd harmonic components of the measured MFL signal spectrum with the plastic strain, where (a) are the measured original values at different points and (b) are the values normalized referring to the amplitude of virgin material (only average value). From the figure, one can find that all the amplitude values of the odd harmonics decrease with the plastic strain. At first, there is a sharply distortion in the signals between the deformation free state and the state of 1% plastic deformation. In range of 1% to 5% plastic strains, all the odd harmonics have a steady but reducing dependence on the plastic deformation. The variation rate of 9th harmonic amplitude is the largest in all the 4 odd super-harmonic components, and the rate may exceed 7% for 5% plastic strain, i.e., the higher odd harmonic is more sensitive to the plastic deformation than the lower harmonics for plastic strain less than 5%.

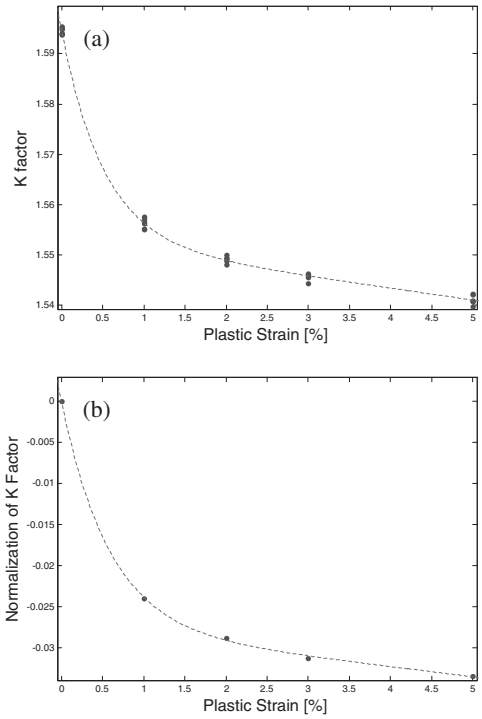

Fig. 18 Correlation of K factor with plastic strain.

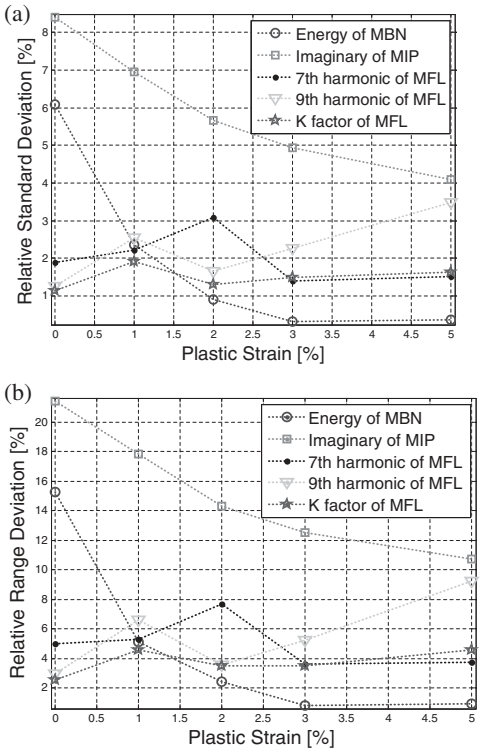

Fig. 19 Relative standard deviation (a) and rang deviation (b) of MBN energy, imaginary peak value of MIP profile, the 7th, 9th and K factor of MFL signals.

Figure 18 gives the results of K factor calculated with eq. (3) from the measured amplitudes of the super-harmonic components. In this case, results at different measurement point are also given in Fig. 18(a), and Fig. 18(b) again gives the normalized average values. Similar results are obtained with the MFL signal amplitude but the correlation can be better fitted with an exponential function for the normalized average values. The experimental results of Fig. 17 and 18 reveal that the MFL signal measurement is also a potential way for the plastic strain evaluation of the SS400 material. Moreover, the result of MFL method is simple and stable, and is robust against the surface status of the test-pieces.

3.4 Discussions

From the measurement results of carbon steel SS400 by MBN, MIP and MFL methods, it can be conclude that the feature parameters such as the energy of MBN signals, the peak value of MIP profile, the amplitude of MFL signals and their corresponding K factor have similar correlation with the residual plastic strain, i.e., all these feature parameters decrease exponentially with the enlarged plastic strains. Consequently, all these three methods show potential ability to evaluate the uni-axial plastic deformation in carbon steel SS400. However, among these evaluated feature parameters, the energy of the MBN signals (when the threshold value is set as the cementite peak), the imaginary peak value of the MIP profile, the 7th and 9th harmonic amplitude and the K factor of MFL signals are more suitable to be adopted for quantitative evaluation of the plastic strain. These feature parameters are not only sensitive to plastic strain smaller than 2%, but also are sensitive to large plastic strain up to 5%. On the other hand, the other parameters such as the peak of real part of MIP profile, 3rd harmonic and 5th harmonic of MFL signals are not as sensitive as others to large plastic strains.

In order to compare the repeatability and reliability of measurement results of the selected feature parameter such as the energy of MBN, the imaginary peak value of MIP profile, the 7th, 9th and the K factor of MFL signals, the relative standard deviation and rang deviation are analyzed based on the following definition formulae

$$RSD = \frac{1}{|\mu_0 - \mu_5|}\sqrt{\frac{1}{N}\sum_{i=1}^{N}(x_i - \mu)^2} \tag{4}$$

$$RRD = \frac{x_{\max} - x_{\min}}{|\mu_0 - \mu_5|} \tag{5}$$

where RSD is the relative standard deviation, RRD is the relative rang deviation, x_i is *i-th* testing data, μ_0 is the average value of virgin test sample and μ_5 is the average value of test sample with plastic strain of 5%, $x_{\max}$ is max value of measured feature parameters and $x_{\min}$ is corresponding minimum value.

Figure 19 gives a comparison of the relative standard deviation and the relative range deviation between the measurement results of MBN, MIP and MFL for different plastic deformation. The results of the relative standard deviation show the dispersion of all testing signals, and the relative range deviation give the range between the maximum to minimum errors. Smaller relative standard deviation and relative range deviation are corresponding to higher measurement reliability and higher measurement accuracy, i.e., the values of the relative standard deviation and relative range deviation can be used to judge the quality of testing results. If a testing result is smaller than the range of deviation, it indicates that this measurement result is not reliable. From Fig. 19, one can find that the MBN energy has noise of

maximum standard deviation up to 6% and range deviation up to 16% even for virgin material. It reveals that the micro-structure of the material show a large inhomogeneous property even for virgin state. It is also can be found that this dispersion in MBN energy signal becomes better once plastic deformation is introduced. On the other hand, both the relative standard deviation and the range deviation of the MIP feature parameter show the largest values among all the feature parameters. The range deviation is large than 10% and some are even as high as 20%. This indicates that the MIP measurement is only suitable for large change of plastic deformation. The major reason of this big deviation may due to that the MIP results are sensitive to the residual magnetic field in material and the ECT pick-up unit is very sensitive to the liftoff. In contrast, the relative standard deviation and the range deviation of the 7th harmonic, 9th harmonic and the K factor of MFL signals are very small, especially the deviation of K factor are small and stable for all the measured plastic deformation. All the relative standard deviation and the relative range error are within 5% for feature parameters of MFL measurements. The results of Fig. 19 reveal that the MFL method is of the best stability, and MIP method shows largest uncertainty.

The MBN, MIP and MFL signals depend on the plastic deformation from the viewpoints of the micro-structures of magnetic domains, magnetic parameter (permeability) and macro leakage magnetic field respectively. Though typical feature parameters of these methods indicate clear and robust correlations with the scale of plastic strain, the different principle makes them show different feature for evaluation of plastic deformation in the carbon steel SS400. The measurement results of the MFL method are of higher stability and repeatability, but of lower space resolution as the MFL signals are average of magnetic field and exciting field of EM magnet nearby the testing point. If the plastic strain is not uniform between the yoke legs, the average processing can limit the space resolution of the measurement results. On the other hand, the MBN method can give better space resolution as the pick-up coil of MBN can be made very small. The disadvantages of MBN method, however, are that it is not suitable for plastic strain of large value and that the relative standard deviation is not small, as the MBN energy is easy to be influenced by the surface quality of test-pieces. The MIP signals are sensitive to the liftoff and remanent magnetization status, which results in a relative larger noise, or lower evaluation precision. Therefore, to develop a system to measure the feature parameters of these three methods at the same time and to evaluate the residual strain through fusion of these signals are helpful to enhance the detectability of degradation and the evaluation accuracy of the plastic deformation.

These methods should be applicable to other ferromagnetic steels other than SS400. For instance, we also have applied the carbon steel Q195(GB/T), a typical structural carbon steel of China, as the testing material for the same measurements, and found a similar correlation between the measured signals and plastic deformation. The quantitative correlation may different for different material, but the qualitative trend is the same.

4. Conclusions

The correlations of plastic deformation with NDE signals of magnetic Barkhausen noise, magnetic incremental permeability and magnetic flux leakage methods are investigated via experiments in this paper. The plastic deformations were introduced to the specimens of carbon steel SS400 by single loading procedure. The measurement results show that the plastic deformation can cause significant change of magnetic properties in the carbon steel, and the measured signals of MBN method, incremental permeability and MFL methods depend on the levels of plastic deformation. There is a good possibility to quantitatively evaluate the plastic strain in mechanical structures of SS400 material by using these methods. In addition, as these 3 methods have different features in term of precision and resolution, an integrated testing system and signal fusion may improve the plastic strain evaluation further.

Acknowledgments

The authors would like to thank National Magnetic Confinement Fusion Program of China (Grant.2013GB113005), the Natural Science Foundation of China (Grant No. 51277139, 11321062 and 11342014) and the National Basic Research Program of China (Grant No. 2011CB610303) for funding this study, and this work is partly supported by the JSPS core to core program, “International research core on smart layered materials and structures for energy saving”.

REFERENCES

1) M. Lindgren and T. Lepisto: NDT&E Int. **33** (2000) 426–428.
2) A. Dhar, L. Clapham and D. L. Atherton: NDT&E Int. **34** (2001) 507–514.
3) X. Kleber and A. Vincent: NDT&E Int. **37** (2004) 439–445.
4) J. C. Sanchez, M. F. Campos and L. R. Padovese: J. Magn. Magn. Mater. **324** (2012) 11–14.
5) A. Sorsa, K. Leiviska and S. Santa-aho: NDT&E Int. **46** (2012) 100–106.
6) M. caldas-Morgan and L. R. Padovese: NDT&E Int. **45** (2012) 148–155.
7) L. Mierczak, D. C. Jiles and G. Fantoni: IEEE Trans. Magn. **47** (2011) 459–465.
8) O. Stupakov, T. Uchimoto and T. Takagi: J. Phys. D: Appl. Phys. **43** (2010) 195003.
9) Z. D. Wang, K. Yao and B. Deng: NDT&E Int. **43** (2010) 513–518.
10) J. W. Wilson, G. Y. Tian and S. Barrans: Sensor Actuators **135** (2007) 381–387.
11) L. Dong, B. Xu and S. Dong: NDT&E Int. **42** (2009) 323–327.
12) P. Wang, S. Zhu and G. Y. Tian: 17th World Conference on Nondestructive Testing, China, 25–28 Oct, (2008).
13) S. Xie, Y. Li, W. Cai, H. E. Chen, Z. Chen, T. Takagi, T. Uchimoto and Y. Yoshida: Mater. Trans. **54** (2013) 964–968.
14) A. Shimamoto and H. Ohkawara: Mater. Trans. **49** (2008) 548–553.
15) O. Stupakov, T. Takagi and T. Uchimoto: NDT&E Int. **43** (2010) 671–676.
16) G. Dobmann: Electromagn. Nondestruct. Eval. (XI), IOS press, (2008) 18–25.
17) C. Boller, I. Altpeter and G. Dobmann: Mat.-wiss. u. Werkstofftech. **42** (2011) 269–278.
18) A. Yashan and G. Dobmann: Electromagn. Nondestruct. Eval. (VI), IOS press, (2002) 150–157.
19) I. Altpeter, R. Becker and G. Dobmann: Inverse Problem **18** (2002) 1907–1921.